Quantum Backaction in Analogue Spacetime

Cisco Gooding

LKB, Sorbonne Université, Paris
in collaboration with Nottingham, Vancouver, Vienna

June 25rd, 2025

Outline


ONE DOES NOT SIMPLY OBSERVE A SYSTEM
WITHOUT DISTURBING IT
imgflip.com

Outline

- $(2+1)$ Relativistic Field+Detector Analogy

Outline

- $(2+1)$ Relativistic Field+Detector Analogy
- Perturbative Backaction with Superfluid Helium

Outline

- $(2+1)$ Relativistic Field+Detector Analogy
- Perturbative Backaction with Superfluid Helium
- Non-perturbative Backaction with a BEC

Outline

- $(2+1)$ Relativistic Field+Detector Analogy
- Perturbative Backaction with Superfluid Helium
- Non-perturbative Backaction with a BEC
- Balancing Backaction and Shot Noise:
  The Standard Quantum Limit and Beyond

Classical Observations

PHYSICAL REVIEW LETTERS **126**, 041105 (2021)

Backreaction in an Analogue Black Hole Experiment

Sam Patrick,[1,*] Harry Goodhew,[2,†] Cisco Gooding,[1,‡] and Silke Weinfurtner[1,3,§]
[1]*School of Mathematical Sciences, University of Nottingham, Nottingham NG7 2FD, United Kingdom*
[2]*Institute of Astronomy, University of Cambridge, Cambridge CB3 0HA, United Kingdom*
[3]*Centre for the Mathematics and Theoretical Physics of Quantum Non-Equilibrium Systems, University of Nottingham, Nottingham NG7 2FD, United Kingdom*

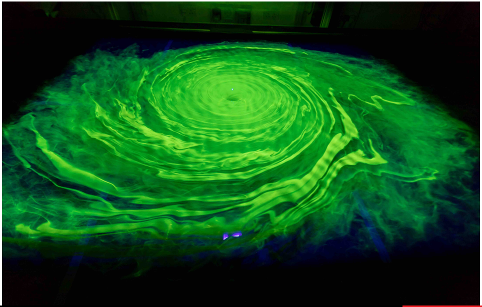

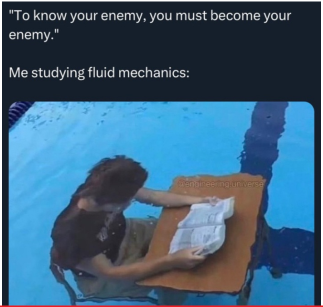

Relativistic Analogy: Superfluid Helium

Thin-film of superfluid helium between the xy-plane ($z = 0$) and $z = h(t, \vec{x}) = h_0 + \eta(t, \vec{x})$ interacts with a laser propagating in the z-direction.

Relativistic Analogy: Superfluid Helium

Thin-film of superfluid helium between the xy-plane ($z = 0$) and $z = h(t, \vec{x}) = h_0 + \eta(t, \vec{x})$ interacts with a laser propagating in the z-direction. Long-wavelength surface fluctuations $\eta(t, \vec{x})$ behave as a $(2 + 1)$ Klein-Gordon field, with quantum interaction Hamiltonian

Relativistic Analogy: Superfluid Helium

Thin-film of superfluid helium between the xy-plane ($z = 0$) and $z = h(t, \vec{x}) = h_0 + \eta(t, \vec{x})$ interacts with a laser propagating in the z-direction. Long-wavelength surface fluctuations $\eta(t, \vec{x})$ behave as a $(2+1)$ Klein-Gordon field, with quantum interaction Hamiltonian

$$\hat{H}_{\mathrm{int}}(t) = \frac{\alpha \rho_N}{2} \hat{E}(t, h_0)^2 \hat{\eta}(t, \vec{X}(t))$$

Relativistic Analogy: Superfluid Helium

Thin-film of superfluid helium between the xy-plane ($z = 0$) and $z = h(t, \vec{x}) = h_0 + \eta(t, \vec{x})$ interacts with a laser propagating in the z-direction. Long-wavelength surface fluctuations $\eta(t, \vec{x})$ behave as a $(2+1)$ Klein-Gordon field, with quantum interaction Hamiltonian

$$\hat{H}_{\mathrm{int}}(t) = \frac{\alpha \rho_N}{2} \hat{E}(t, h_0)^2 \hat{\eta}(t, \vec{X}(t))$$

The laser is described by an electric field

$$\hat{E}(t, z) = \sqrt{\frac{\hbar \omega_0}{4\pi\varepsilon_0 c A_\perp}} \left[E_0(t, z) + \delta \hat{E}(t, z) \right]$$

Relativistic Analogy: Superfluid Helium

Thin-film of superfluid helium between the xy-plane ($z = 0$) and $z = h(t, \vec{x}) = h_0 + \eta(t, \vec{x})$ interacts with a laser propagating in the z-direction. Long-wavelength surface fluctuations $\eta(t, \vec{x})$ behave as a $(2+1)$ Klein-Gordon field, with quantum interaction Hamiltonian

$$\hat{H}_{\rm int}(t) = \frac{\alpha \rho_N}{2} \hat{E}(t, h_0)^2 \hat{\eta}(t, \vec{X}(t))$$

The laser is described by an electric field

$$\hat{E}(t, z) = \sqrt{\frac{\hbar\omega_0}{4\pi\varepsilon_0 c A_\perp}} \left[E_0(t, z) + \delta\hat{E}(t, z) \right]$$

with coherent amplitude

$$E_0(t, z) = a_0(t - z) \mathrm{e}^{-i\omega_0(t-z)} + c.c.$$

Relativistic Analogy: Superfluid Helium

Thin-film of superfluid helium between the xy-plane ($z = 0$) and $z = h(t, \vec{x}) = h_0 + \eta(t, \vec{x})$ interacts with a laser propagating in the z-direction. Long-wavelength surface fluctuations $\eta(t, \vec{x})$ behave as a $(2+1)$ Klein-Gordon field, with quantum interaction Hamiltonian

$$\hat{H}_{\text{int}}(t) = \frac{\alpha \rho_N}{2} \hat{E}(t, h_0)^2 \hat{\eta}(t, \vec{X}(t))$$

The laser is described by an electric field

$$\hat{E}(t, z) = \sqrt{\frac{\hbar \omega_0}{4\pi \varepsilon_0 c A_\perp}} \left[E_0(t, z) + \delta \hat{E}(t, z) \right]$$

with coherent amplitude

$$E_0(t, z) = a_0(t - z) \mathrm{e}^{-i\omega_0 (t-z)} + c.c.$$

and (vacuum) fluctuations

$$\delta \hat{E}(t, z) = \mathrm{e}^{-i\omega_0 (t-z)} \int_{-\Delta}^{\Delta} \frac{\mathrm{d}\nu}{2\pi} \mathrm{e}^{-i\nu (t-z)} \delta \hat{a}_\nu + h.c.$$

Effective Unruh-DeWitt Detectors

Effective Unruh-DeWitt Detectors

Neglecting rapidly oscillating terms, the linear part of $(E_0 + \delta\hat{E})^2$ becomes

$$E_0 \delta\hat{E} \approx a_0(t - z) \int_{-\Delta}^{\Delta} \frac{\mathrm{d}\nu}{2\pi} \mathrm{e}^{-i\nu(t-z)} \delta\hat{a}_\nu + h.c.$$

Effective Unruh-DeWitt Detectors

Neglecting rapidly oscillating terms, the linear part of $(E_0 + \delta\hat{E})^2$ becomes

$$E_0 \delta\hat{E} \approx a_0(t-z) \int_{-\Delta}^{\Delta} \frac{\mathrm{d}\nu}{2\pi} \mathrm{e}^{-i\nu(t-z)} \delta\hat{a}_\nu + h.c.$$

Hence, suppressing the evaluation at $z = h_0$, we obtain

$$\mathcal{H}_{\mathrm{int}}(t) \approx \lambda\, a_0(t)\, \hat{\mu}(t)\, \hat{\eta}(t, \vec{X}(t))\,,$$

analogous to the Unruh-DeWitt detector model, with switching function $a_0(t)$, $(2+1)$-dimensional quantum field $\hat{\eta}(t, \vec{X}(t))$, and coupling constant

$$\lambda = \frac{\alpha \rho_N \hbar\omega_0}{4\pi\varepsilon_0 c A_\perp},$$

Effective Unruh-DeWitt Detectors

Neglecting rapidly oscillating terms, the linear part of $(E_0 + \delta\hat{E})^2$ becomes

$$E_0\delta\hat{E} \approx a_0(t-z)\int_{-\Delta}^{\Delta}\frac{\mathrm{d}\nu}{2\pi}\mathrm{e}^{-i\nu(t-z)}\delta\hat{a}_\nu + h.c.$$

Hence, suppressing the evaluation at $z = h_0$, we obtain

$$\mathcal{H}_{\mathrm{int}}(t) \approx \lambda\, a_0(t)\,\hat{\mu}(t)\,\hat{\eta}(t,\vec{X}(t))\,,$$

analogous to the Unruh-DeWitt detector model, with switching function $a_0(t)$, $(2+1)$-dimensional quantum field $\hat{\eta}(t,\vec{X}(t))$, and coupling constant

$$\lambda = \frac{\alpha\rho_N\hbar\omega_0}{4\pi\varepsilon_0 cA_\perp},$$

with a monopole moment operator $\hat{\mu}(t)$ that is a **continuum of Unruh-DeWitt detectors with energy gaps** $\nu \in [-\Delta,\Delta]$**:**

$$\hat{\mu}(t) = \int_{-\Delta}^{\Delta}\frac{\mathrm{d}\nu}{2\pi}\left(\delta\hat{a}_\nu\mathrm{e}^{-i\nu t} + \delta\hat{a}_\nu^\dagger\mathrm{e}^{i\nu t}\right).$$

Interaction-picture Perturbations (c.f. Leo)

Time evolution operator $\hat{U}(t_f) = \mathcal{T}\exp\left(-\mathrm{i}\int_{-\infty}^{t_f} \hat{H}_{\text{int}}(t)\,\mathrm{d}t\right)$, such that $\hat{\rho}_f = \hat{U}(t_f)\hat{\rho}_i\hat{U}^\dagger(t_f) = \hat{\rho}_i + \hat{\rho}_f^{(1)} + \hat{\rho}_f^{(2)} \ldots$.

$$\hat{\rho}_f^{(1)} = -\mathrm{i}\int_{-\infty}^{t_f} \mathrm{d}x \left[\hat{H}_{\text{int}}(x), \hat{\rho}_i\right]$$

$$\hat{\rho}_f^{(2)} = \int_{-\infty}^{t_f} \mathrm{d}x \int_{-\infty}^{x} \mathrm{d}x' \left[\left[\hat{H}_{\text{int}}(x), \hat{\rho}_i\right], \hat{H}_{\text{int}}(x')\right].$$

If we assume an initially uncorrelated state $\hat{\rho}_i = \hat{\rho}_{i,E} \otimes \hat{\rho}_{i,\eta}$, and trace over the electric field to focus on the final state of the fluid height, we find

$$\hat{\rho}_{f,\eta}^{(1)} = -\mathrm{i}\frac{\alpha\rho_N}{2}\int_{-\infty}^{t_f} \mathrm{d}t' \left[\hat{\eta}_{\vec{X}}(t'), \hat{\rho}_{i,\eta}\right]\langle\hat{E}(t')^2\rangle_i$$

which we use to find the expectation value of the fluid height

$$\langle\hat{\eta}(t,\vec{x})\rangle_f = \frac{\alpha\rho_N}{2}\int_{-\infty}^{t} \mathrm{d}t'\, G_R(t', \vec{X}(t); t, \vec{x})\langle\hat{E}(t')^2\rangle_i.$$

Field Correlations

Using the notation $\mathrm{x} = (t, \vec{x})$ and the assumption that the initial state of the fluid surface is thermal, we find

Field Correlations

Using the notation $\mathrm{x} = (t, \vec{x})$ and the assumption that the initial state of the fluid surface is thermal, we find

$$\langle \hat{\eta}(\mathrm{x})\hat{\eta}(\mathrm{x}')\rangle_{\mathrm{f}} = \frac{\alpha^2 \rho_N^2}{4} \operatorname{Im}\left[\int_{-\infty}^{t} \mathrm{d}q G_R(q, \vec{X}(q); \mathrm{x}) \mathcal{A}(q; \mathrm{x}')\right]$$

$$\mathcal{A}(q; \mathrm{x}') = \int_{-\infty}^{q} \mathrm{d}p \langle \hat{\eta}(p, \vec{X}(p))\hat{\eta}(\mathrm{x}')\rangle_i \langle \hat{E}(p)^2 \hat{E}(q)^2\rangle_i.$$

$$\langle \hat{\eta}(\mathrm{x})\hat{\eta}(\mathrm{x}')\rangle_{\mathrm{f}} = \langle \hat{\eta}(\mathrm{x})\hat{\eta}(\mathrm{x}')\rangle_{\mathrm{f}}^{E_0} + \langle \hat{\eta}(\mathrm{x})\hat{\eta}(\mathrm{x}')\rangle_{\mathrm{f}}^{\delta E} + \mathcal{O}(\delta \hat{E}^4)$$

Field Correlations

Using the notation $\mathrm{x} = (t, \vec{x})$ and the assumption that the initial state of the fluid surface is thermal, we find

$$\langle\hat{\eta}(\mathrm{x})\hat{\eta}(\mathrm{x}')\rangle_{\mathrm{f}} = \frac{\alpha^2\rho_N^2}{4}\,\mathrm{Im}\left[\int_{-\infty}^{t}\mathrm{d}q G_R(q,\vec{X}(q);\mathrm{x})\mathcal{A}(q;\mathrm{x}')\right]$$

$$\mathcal{A}(q;\mathrm{x}') = \int_{-\infty}^{q}\mathrm{d}p\langle\hat{\eta}(p,\vec{X}(p))\hat{\eta}(\mathrm{x}')\rangle_i\langle\hat{E}(p)^2\hat{E}(q)^2\rangle_i.$$

$$\langle\hat{\eta}(\mathrm{x})\hat{\eta}(\mathrm{x}')\rangle_{\mathrm{f}} = \langle\hat{\eta}(\mathrm{x})\hat{\eta}(\mathrm{x}')\rangle_{\mathrm{f}}^{E_0} + \langle\hat{\eta}(\mathrm{x})\hat{\eta}(\mathrm{x}')\rangle_{\mathrm{f}}^{\delta E} + \mathcal{O}(\delta\hat{E}^4)$$

Spectrum of Unruh-DeWitt detectors with energy gap $E = \nu$:

$$\langle\hat{\eta}(\mathrm{x})\hat{\eta}(\mathrm{x}')\rangle_{\mathrm{f}} = \lambda^2\int_{-\Delta}^{\Delta}\frac{\mathrm{d}\nu}{4\pi^2}B(\mathrm{x},\mathrm{x}',\nu)$$

where in the coincidence limit we have

$$B(\mathrm{x},\mathrm{x},\nu) = \left|\int_{-\infty}^{\infty}\mathrm{d}t' a_0(t')G_R(\mathrm{x},\vec{Z}(t'))\mathrm{e}^{-i\nu t'}\right|^2$$

Classical and Quantum Variance

Re-writing a_0 in terms of a dimensionless $\chi \in [0,1]$ such that the maximum laser power is $P_{\max}$, we obtain the standard switching:

$$\chi(\tau) := a_0(\tau)\sqrt{\frac{\hbar\omega_0}{P_{\max}}}.$$

Relevant quantities to compare scales for classical and quantum fluctuations:

$$\frac{\mathrm{Var}(\hat{\eta})}{\lambda^2} = \frac{P_{\max}}{\hbar\omega_0}\int_{-\Delta}^{\Delta}\frac{\mathrm{d}\nu}{4\pi^2}\left|\int_{-\infty}^{\infty}\mathrm{d}t'\chi(t')G_R(\mathsf{x},\mathsf{Z}(t'))\mathrm{e}^{i\nu t'}\right|^2$$

$$\frac{\eta_{\mathrm{class}}(\mathsf{x})^2}{\lambda^2} = \left(\frac{P_{\max}}{\hbar\omega_0}\right)^2\left[\int_{-\infty}^{\infty}\mathrm{d}t' G_R(\mathsf{x},\mathsf{Z}(t'))\chi(t')^2\right]^2$$

Overall scaling indicates dominance of classical backaction at high laser powers (/high photon rates)

Variance Comparison: Static Case

Backaction variances for frequency band width $\Delta = (2\pi)1.2\text{KHz}$ and photon rate at time of measurement $\zeta := \frac{P_{\max}}{\hbar\omega_0} = 10\text{Hz}$.

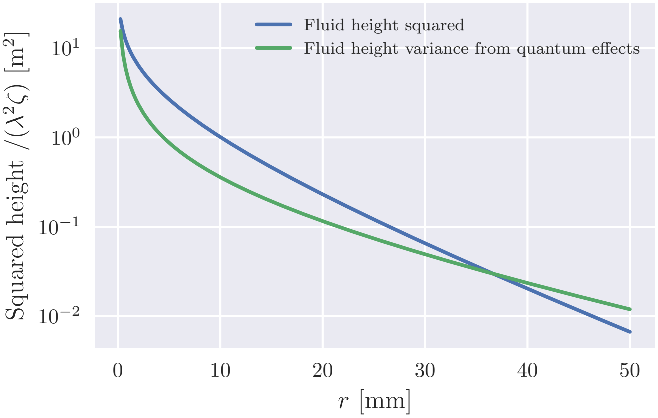

Circular Interaction Trajectories (c.f. Adam's numerics)

The squared average fluid height (left-left) alongside the variance in the fluid height as a result of electromagnetic fluctuations (left-right) for a circular trajectory of radius 5mm at a speed of 0.9 times the speed of surface waves in the superfluid helium.

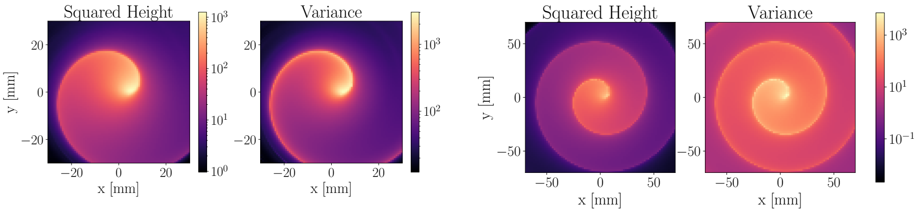

Rightmost: radius 5mm at a speed of 0.9 times the speed of surface waves in the superfluid helium. Slower fall-off of the variance at larger distances from the laser trajectory. ($\Delta = (2\pi)1.2$ KHz, $\zeta = 10\text{s}^{-1}$, $a = 2\text{s}^{-1}$).

Laser-coupled BECs (à la Jorma's talk)

Experimental Proposal: Focusing a laser onto a pancake BEC with a moving interaction point allows the “vacuum” to be probed along an accelerated trajectory [C. Gooding et al. **PRL.125.213603(2020)**].

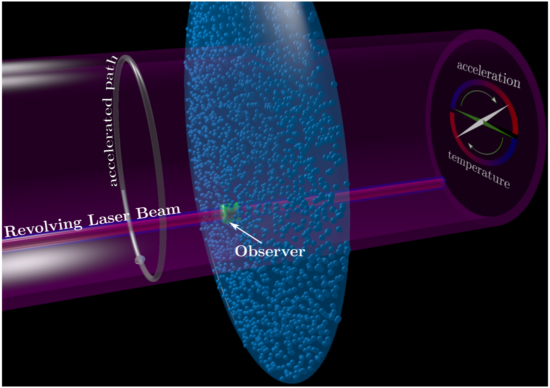

Relativistic Field and Response Function

BEC density fluctuations behave as an effective relativistic field, sampled by a laser along the interaction trajectory:

$$\phi(t, \vec{X}(t)) \;\equiv\; \phi(t) \;=\; \int_{-\Delta}^{\Delta} \frac{d\nu}{2\pi} e^{-i\nu t} D_\nu \,,$$

where D_ν is the annihilation (creation) operator for positive (negative) frequency modes with respect to the accelerating detector. The **accelerated-detector response function** takes the form

$$S_{\phi\phi}[\nu] \;=\; \int dt\, e^{-i\nu t} \langle \phi(t)\phi(0) \rangle \,.$$

Our signal is the Fourier transform of the Wightman function for the BEC field, pulled back to the interaction trajectory.

Experimental Setup (à l'optomécanique)

The detector response function can be extracted by splitting and heterodyning a pair of modulation bands shifted by Ω from an atomic resonance at ω_0:

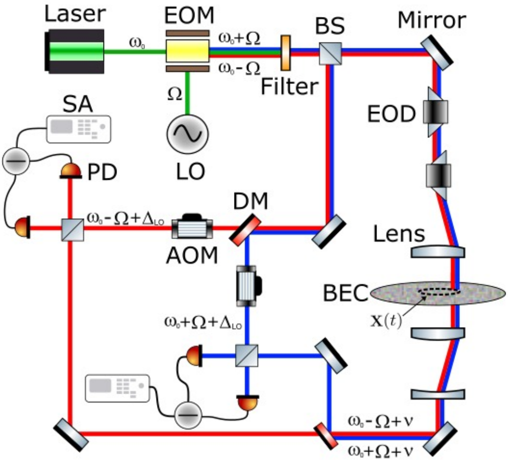

Nonperturbative Backaction [JLoTempPhys208.196(2022)]

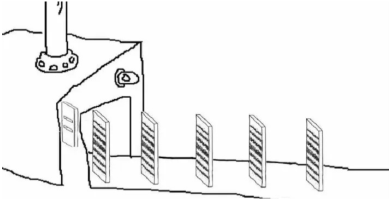

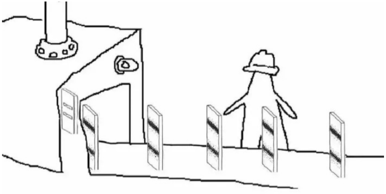

Laser fluctuations at frequencies $\omega_0 \pm \Omega + \nu$ (c.f. Bill's Bogoliubov method):

$$\delta\tilde{a}_{\pm}[\nu] \; = \; \delta a_{\pm}[\nu] \pm \frac{i\mu D_{\nu}}{\sqrt{2}} \pm \frac{\mu^2}{4}\mathrm{sgn}(\nu)\delta a_b[\nu]\,,$$

where $\mu \equiv -\varepsilon\alpha/\sqrt{2}$ is a laser-enhanced coupling parameter and the quantum backaction takes the explicit form

$$\delta a_b[\nu] = \delta a_-[\nu] + \delta a_-[-\nu]^\dagger - \delta a_+[\nu] - \delta a_+[-\nu]^\dagger\,.$$

Dual-arm Heterodyne Detection

The complete signal can be extracted by splitting and heterodyning the pair of modulation bands (heterodyne detetuning Δ_{LO}):

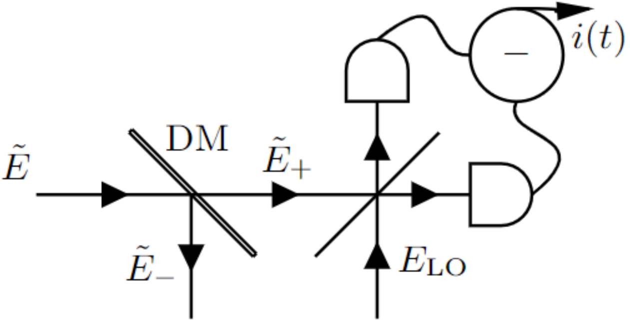

FIG. 1. Heterodyne detection scheme. Dichroic mirror labelled DM.

Photocurrent PSD Inferred Signal

Photocurrent PSD Inferred Signal

Difference photon flux (measured):

Photocurrent PSD Inferred Signal

Difference photon flux (measured):

$$n(t) \equiv 2\alpha|\beta|\cos(\Delta_{LO}t) + |\beta|\left(e^{i\Delta_{LO}t}\delta\tilde{a}_+(t) + e^{-i\Delta_{LO}t}\delta\tilde{a}_+(t)^\dagger\right) .$$

Photocurrent PSD Inferred Signal

Difference photon flux (measured):

$$n(t) \equiv 2\alpha|\beta|\cos(\Delta_{LO}t) + |\beta|\left(e^{i\Delta_{LO}t}\delta\tilde{a}_{+}(t) + e^{-i\Delta_{LO}t}\delta\tilde{a}_{+}(t)^{\dagger}\right) .$$

The difference photocurrent power spectral density (PSD):

Photocurrent PSD Inferred Signal

Difference photon flux (measured):

$$n(t) \equiv 2\alpha|\beta|\cos(\Delta_{LO}t) + |\beta|\left(e^{i\Delta_{LO}t}\delta\tilde{a}_+(t) + e^{-i\Delta_{LO}t}\delta\tilde{a}_+(t)^\dagger\right) .$$

The difference photocurrent power spectral density (PSD):

$$S_{ii}[\Delta_{LO} - \nu] = 1 + \frac{\mu^2}{2}\left(S_{\phi\phi}[\nu] - \mathrm{sgn}(\nu)\right) + \frac{\mu^4}{8}$$

Photocurrent PSD Inferred Signal

Difference photon flux (measured):

$$n(t) \quad \equiv \quad 2\alpha|\beta|\cos(\Delta_{LO}t) + |\beta|\left(e^{i\Delta_{LO}t}\delta\tilde{a}_{+}(t) + e^{-i\Delta_{LO}t}\delta\tilde{a}_{+}(t)^{\dagger}\right) .$$

The difference photocurrent power spectral density (PSD):

$$S_{ii}[\Delta_{LO} - \nu] \; = \; 1 + \frac{\mu^2}{2}\left(S_{\phi\phi}[\nu] - \mathrm{sgn}(\nu)\right) + \frac{\mu^4}{8}$$

Rescaling by $2/\mu^2$ to refer the normalised difference photocurrent back to the signal, we obtain the *inferred* PSD signal

Photocurrent PSD Inferred Signal

Difference photon flux (measured):

$$n(t) \equiv 2\alpha|\beta|\cos(\Delta_{LO}t) + |\beta|\left(e^{i\Delta_{LO}t}\delta\tilde{a}_+(t) + e^{-i\Delta_{LO}t}\delta\tilde{a}_+(t)^\dagger\right) .$$

The difference photocurrent power spectral density (PSD):

$$S_{ii}[\Delta_{LO} - \nu] = 1 + \frac{\mu^2}{2}\left(S_{\phi\phi}[\nu] - \mathrm{sgn}(\nu)\right) + \frac{\mu^4}{8}$$

Rescaling by $2/\mu^2$ to refer the normalised difference photocurrent back to the signal, we obtain the *inferred* PSD signal

$$S^{inf}_{\phi\phi}[\nu] = S_{\phi\phi}[\nu] + \mathcal{N}[\nu] ,$$

Photocurrent PSD Inferred Signal

Difference photon flux (measured):

$$n(t) \equiv 2\alpha|\beta|\cos(\Delta_{LO}t) + |\beta|\left(e^{i\Delta_{LO}t}\delta\tilde{a}_{+}(t) + e^{-i\Delta_{LO}t}\delta\tilde{a}_{+}(t)^{\dagger}\right).$$

The difference photocurrent power spectral density (PSD):

$$S_{ii}[\Delta_{LO}-\nu] = 1 + \frac{\mu^2}{2}\left(S_{\phi\phi}[\nu] - \mathrm{sgn}(\nu)\right) + \frac{\mu^4}{8}$$

Rescaling by $2/\mu^2$ to refer the normalised difference photocurrent back to the signal, we obtain the *inferred* PSD signal

$$S_{\phi\phi}^{inf}[\nu] = S_{\phi\phi}[\nu] + \mathcal{N}[\nu],$$

where the *added noise* PSD is defined by

Photocurrent PSD Inferred Signal

Difference photon flux (measured):

$$n(t) \equiv 2\alpha|\beta|\cos(\Delta_{LO}t) + |\beta|\left(e^{i\Delta_{LO}t}\delta\tilde{a}_+(t) + e^{-i\Delta_{LO}t}\delta\tilde{a}_+(t)^\dagger\right).$$

The difference photocurrent power spectral density (PSD):

$$S_{ii}[\Delta_{LO} - \nu] = 1 + \frac{\mu^2}{2}\left(S_{\phi\phi}[\nu] - \mathrm{sgn}(\nu)\right) + \frac{\mu^4}{8}$$

Rescaling by $2/\mu^2$ to refer the normalised difference photocurrent back to the signal, we obtain the *inferred* PSD signal

$$S^{inf}_{\phi\phi}[\nu] = S_{\phi\phi}[\nu] + \mathcal{N}[\nu],$$

where the *added noise* PSD is defined by

$$\mathcal{N}[\nu] = \frac{2}{\mu^2} + \frac{\mu^2}{4} - \mathrm{sgn}(\nu).$$

The Standard Quantum Limit

The added noise PSD attains its minimum when $\mu^2 = 2\sqrt{2}$, which corresponds to $\alpha_{SQL}^2 = 4\sqrt{2}/\varepsilon^2$ (with $\varepsilon = 2|\hat{\alpha}_R|\omega_0\sqrt{m\rho_0}$, where $\hat{\alpha}_R$ is the real part of the atomic polarisability, ω_0 is the central laser frequency, m is the atomic mass, and ρ_0 is the background BEC density). This corresponds to a laser power $P_{SQL} = 8\sqrt{2}\omega_0/\varepsilon^2$, averaged over modulation cycles.
The added noise at the SQL is

$$\mathcal{N}[\nu] = \sqrt{2} - \mathrm{sgn}(\nu)\,.$$

Squeezing Difference-modes in the EM Field

Like LIGO, shot-noise dominates the *added noise* at low laser powers, and backaction dominates at high powers. Backaction noise can be suppressed by squeezing the initial laser field, at the cost of increasing noise in the signal carrier:

$$\mathcal{N}(\nu, \mu, \lambda) = \frac{1}{\mu^2}\left(1 + \cosh^2\lambda\right) + \frac{\mu^2\, e^{-2\lambda}}{4} - e^{-\lambda}\mathrm{sgn}(\nu)$$

For fixed squeezing parameter λ, the added noise is minimal for $\mu_\lambda^2 = 2e^\lambda\sqrt{1+\cosh^2\lambda}$. The resulting added noise $\mathcal{N}(\nu, \mu_\lambda, \lambda)$ (with $\nu > 0$) is then minimal for $\lambda = \frac{1}{2}\ln\left(\sqrt{5}+2\right) \approx 0.7218$.

Beating the Standard Quantum Limit

Further paralleling LIGO, squeezing the initial laser probe allows the SQL to be beaten (thanks for plotting, Cameron!):

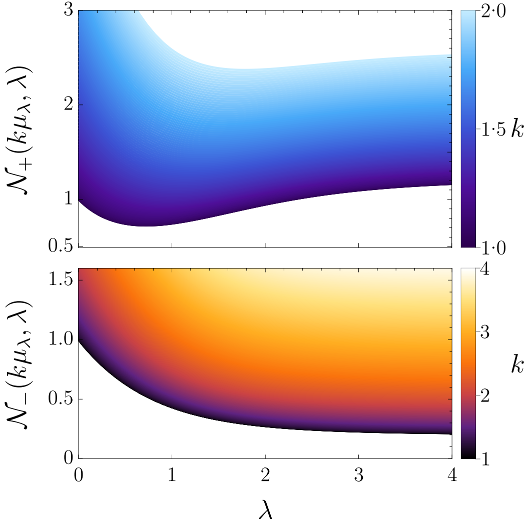

Will it cook the pancake BEC in the process?

To ensure a nondestructive measurement, the photon scattering rate per atom, $\Gamma_{\mathrm{sc}} = 4\hat{\alpha}_I \bar{P}/\pi r_0^2$, should be much less than unity. Here, $\hat{\alpha}_I$ is the imaginary part of the atomic polarisability, r_0 is the laser spot size, and $\bar{P} \approx 2\omega_0\alpha^2$ is the laser power.

Now, considering the ratio $\bar{P}/2\omega_0\alpha_{SQL}^2$, reaching the SQL corresponds to $\Gamma_{\mathrm{sc}} \approx 0.0035\mathrm{Hz}$.

Will it cook the pancake BEC in the process?

To ensure a nondestructive measurement, the photon scattering rate per atom, $\Gamma_{\rm sc} = 4\hat{\alpha}_I \bar{P}/\pi r_0^2$, should be much less than unity. Here, $\hat{\alpha}_I$ is the imaginary part of the atomic polarisability, r_0 is the laser spot size, and $\bar{P} \approx 2\omega_0 \alpha^2$ is the laser power.

Now, considering the ratio $\bar{P}/2\omega_0\alpha_{SQL}^2$, reaching the SQL corresponds to $\Gamma_{\rm sc} \approx 0.0035$Hz.

To optimally beat the SQL with squeezing, we consider $\lambda = \frac{1}{2}\ln\left(\sqrt{5}+2\right) \approx 0.7218$, in which case the photon scattering rate becomes $\Gamma_{\rm sc} \approx 0.012$Hz.

Will it cook the pancake BEC in the process?

To ensure a nondestructive measurement, the photon scattering rate per atom, $\Gamma_{\rm sc} = 4\hat{\alpha}_I \bar{P}/\pi r_0^2$, should be much less than unity. Here, $\hat{\alpha}_I$ is the imaginary part of the atomic polarisability, r_0 is the laser spot size, and $\bar{P} \approx 2\omega_0\alpha^2$ is the laser power.

Now, considering the ratio $\bar{P}/2\omega_0\alpha_{SQL}^2$, reaching the SQL corresponds to $\Gamma_{\rm sc} \approx 0.0035$Hz.

To optimally beat the SQL with squeezing, we consider $\lambda = \frac{1}{2}\ln\left(\sqrt{5}+2\right) \approx 0.7218$, in which case the photon scattering rate becomes $\Gamma_{\rm sc} \approx 0.012$Hz.

Conclusion: The SQL can be both reached and optimally beaten to “cook the steak” without cooking the pancake!

Ringraziamenti

Thanks to Adam, Leo, Jorma, Silke, Bill, Jörg, Sebastian, Samin, Cameron, and the rest of the Gravity Laboratory team (Chris, not shown: thanks for the figure!)